Long Noncoding RNA SGO1-AS1 Inactivates TGFβ Signaling by Facilitating TGFB mRNA Decay and Inhibits Gastric Carcinoma Metastasis

Donglan Huang (donglanhuang@gzhmu.edu.cn)
Guangzhou Medical University Affiliated Cancer Hospital https://orcid.org/0000-0002-2585-0568
Ke Zhang
Guangzhou Medical University
Wenying Zheng
Guangzhou Medical University
Ruixin Zhang
Guangzhou Medical University
Jiale Chen
Guangzhou Medical University
Nan Du
Sun Yat-sen University Cancer Center
Yuanyuan Xia
Guangzhou Medical University
Yan Long
Guangzhou Women and Children's Medical Center
Yixue Gu
Guangzhou Medical University
Jianhua Xu
Guangzhou University of Chinese Medicine
Min Deng
Guangzhou Medical University

Research

Keywords: gastric carcinoma, metastasis, lncRNA, SGO1-AS1, TGFβ, ZEB1

Posted Date: May 17th, 2021

DOI: https://doi.org/10.21203/rs.3.rs-523089/v1

Abstract

Background: Although thousands of long noncoding RNAs (lncRNAs) have been annotated, only a limited number of them have been characterized functionally. In this study, we aimed to identify novel lncRNAs involved in the progression of gastric carcinoma (GC) and explore their regulatory mechanisms and clinical significance in GC.

Methods: LncRNA expression microarray was used to identify differential lncRNA expression profiles between paired GCs and adjacent normal mucosa tissues. Using the above method, lncRNA SGO1-AS1 was picked out for further study. Quantitative reverse transcription polymerase chain reaction (qRT-PCR) and in situ hybridization (ISH) were performed to detect SGO1-AS1 expression in GC tissues. Gain-of-function and loss-of-function analyses were performed to investigate the functions of SGO1-AS1 and its upstream and downstream regulatory mechanisms *in vitro* and *in vivo*.

Results: SGO1-AS1 was downregulated in gastric carcinoma tissues compared to adjacent normal tissues, and its downregulation was positively correlated with advanced clinical stage, metastasis status and poor patient prognosis. Functional experiments revealed that SGO1-AS1 inhibited GC cell invasion and metastasis *in vitro* and *in vivo*. Mechanistically, SGO1-AS1 facilitated TGFB1/2 mRNA decay by competitively binding the PTBP1 protein, which resulted in reduced TGFβ production and thus prevented the epithelial-to-mesenchymal transition (EMT) and metastasis. In addition, TGFβ in turn could inhibited SGO1-AS1 transcription by inducing ZEB1. Thus, SGO1-AS1 and TGFβ form a double-negative feedback loop via ZEB1 to regulate EMT and metastasis.

Conclusions: SGO1-AS1 functions as an endogenous inhibitor of the TGFβ pathway and suppresses gastric carcinoma metastasis, indicating a novel potential target for GC treatment.

Background

Gastric carcinoma is one of the most common malignancies worldwide and the fourth leading cause of cancer death [1]. Approximately 40% of patients with gastric carcinoma present with metastases, and only about 5% of these patients exhibit 5-year survival [2]. The prognosis of GC patients with metastatic disease remains poor due to the lack of effective therapies. New therapeutic options will become available only if we improve our understanding of the mechanisms underlying metastatic spread.

LncRNAs are transcripts longer than 200 nucleotides without protein-coding potential [3]. Tens of thousands of lncRNAs are expressed in human cells, but the function of a large majority of them remains unknown [4]. An increasing number of studies have demonstrated the importance of lncRNAs for regulating a wide range of processes, including development, differentiation, cell proliferation, cell death and cancer development [5, 6]. Recently, several GC-implicated lncRNAs have been identified, and their functions and mechanisms have been clarified [7–11]. For instance, the lncRNA GClnc1 promotes gastric carcinogenesis and may act as a scaffold for WDR5 and KAT2A complexes to specify the histone modification pattern [9]. The lncRNA GMAN enhances the translation of ephrin A1 mRNA by binding

competitively to GMAN-AS and thus promotes GC invasion and metastasis [10]. However, the well-characterized lncRNAs that are involved in GC are merely the tip of the iceberg and an even larger number remain unknown.

Here, we demonstrated that the lncRNA SGO1-AS1 (also known as SGOL1-AS1), which is downregulated in gastric carcinoma and associated with tumor progression and patient prognosis, prevents gastric carcinoma EMT, invasion and metastasis *in vitro* and *in vivo*. Mechanistically, SGO1-AS1 reduces the stability of TGFB1/2 mRNA by competitively binding PTBP1 protein, resulting in reduced TGFβ production. TGFβ, in turn, inhibits SGO1-AS1 transcription by inducing ZEB1. Thus, in this study, we identified a novel metastasis-suppressive lncRNA, SGO1-AS1, with crucial biological, mechanistic and clinical impacts on GC, mediating a double-negative feedback loop with TGFβ via ZEB1.

Methods

Clinical specimens

Five pairs of snap-frozen GC tissues and matched adjacent normal mucosa tissues were obtained for lncRNA microarray analysis. Furthermore, two cohorts of frozen samples used for qRT-PCR assay were collected: a small GC cohort (Cohort 1) contained 18 pairs of GC tissues and corresponding adjacent normal mucosa tissues to confirm 13 lncRNAs with more than a 4-fold difference in microarray analysis; and a large GC cohort (Cohort 2) included 92 pairs of GC tissues and matched adjacent normal samples to detect the expression levels of SGO1-AS1, TGFB1/2 and ZEB1. Additionally, GC tissue microarrays containing 95 GC tissues and 80 adjacent tissues (Cohort 3) used for ISH analysis were enrolled for this study. All tissues were collected immediately after surgery from the Affiliated Cancer Hospital of Guangzhou Medical University (Guangzhou, Guangdong, China). The clinical and histopathological characteristics for the patients are described in Additional file 1: Table S1-2.

Microarray analysis

Total RNA was extracted from 5 paired GC tissues and corresponding adjacent normal mucosa tissues using the TRIZOL reagent (Invitrogen, Carlsbad, CA, USA) according to the manufacturer's instructions. Total RNA was amplified and reverse-transcribed into fluorescent cDNA. The labeled cDNA was then hybridized onto the LncRNA + mRNA Human Gene Expression Microarray V4.0 (Agilent, Palo Alto, CA), and after washing, the arrays were scanned with an Agilent Scanner G2565CA (Agilent). Agilent Feature Extraction software (version 10.7.3.1) was used to analyze the acquired array images and the Agilent qRT-PCR results. Data are available via gene expression omnibus (GEO) under accession number GSE157289.

qRT-PCR

Total RNA was isolated from patient tissues and cultured cells using TRIzol reagent (Invitrogen) and cDNA was synthesized using the PrimeScript RT Reagent Kit (Takara, Otsu, Japan). Subsequent quantitative polymerase chain reaction (qPCR) analyses were performed using the SYBR Premix Ex Taq

Kit (Applied Biosystems, Foster City, CA, USA). β-actin was used as the endogenous control to normalize gene expression. The primer sequences for each gene are provided in Additional file 1: Table S3.

In situ hybridization

ISH analysis was performed using a kit from Boster (Wuhan, Hubei, China). Tissue microarray slides were deparaffinized, digested with proteinase K, hybridized with DIG-labeled probes for SGO1-AS1 and U6 at 52℃ overnight and subsequently visualized with an anti-DIG-POD antibody and DAB complex. The SGO1-AS1 probe was 5′- CCGCCTCCCAGCCAACCAATGGAGGAGCGAGGCG-3′. We quantitatively scored the tissue sections based on the percentage of positively stained cells and staining intensity.

Rapid amplification of cDNA ends (RACE) analysis

We used the 5′-RACE and 3′-RACE analyses to determine the transcriptional initiation and termination sites of SGO1-AS1 using a SMARTer™ RACE cDNA Amplification Kit (Clontech, Palo Alto, CA, USA), following the manufacturer's instructions. Nested PCR products were cloned into pMD20-T vector and then sequenced. The sequences of SGO1-AS1 specific primers used in nested PCR of RACE assay are shown in Additional file 1: Table S4.

Subcellular fractionation

Nuclear and cytoplasmic separation was performed using the PARIS Kit (Life Technologies, USA) according to the manufacturer's instructions, and then qRT-PCR analysis was conducted.

Cell culture

The GC cell lines SGC7901, BGC823, AGS, MGC803, MKN45 and MKN28 were obtained from the Chinese Academy of Medical Science (Beijing, China), and the gastric epithelial cell line GES-1 were obtained from the Beijing Institute for Cancer Research (Beijing, China). The GC cell line NCI-N87 and the HEK293T cell line were obtained from the American Type Culture Collection (Manassas VA, USA). The cell lines involved in our experiments were reauthenticated by short tandem repeat analysis every 6 months after resuscitation in our laboratory. These cells were cultured in Dulbecco's Modified Eagle's Medium (DMEM, Gibco, USA) supplemented with 10% fetal bovine serum (Gibco) at 37℃ in 5% CO_2.

RNAi, plasmid construction and cell transfection

The recombinant lentiviral vectors for SGO1-AS1 overexpression or knockdown were purchased from RiboBio (Guangzhou, Guangdong, China), and PTBP1 short hairpin RNA (shRNA) lentiviral vectors were obtained from GeneChem (Shanghai, China). The target sequences for SGO1-AS1 and PTBP1 were as follows: shAS1#1, 5′-GCTATCTTCCTCCTCCTCACA-3′; shAS1#2, 5′-CTACCGCCGCCACATTCGAAA-3′; shAS1#3, 5′-GCCTCCCTCTTGTGAGAAGAA-3′; shAS1#4, 5′-AGCTTGCAACGCGGAAGCAGC-3′; and shPTBP1, 5′-GCGGCCAGCC CATCTACATC-3′. To establish the cell lines that stably overexpress or deplete SGO1-AS1, SGC-7901 cells were infected with recombinant SGO1-AS1 lentiviruses, while MKN28 cells were infected with SGO1-AS1 shRNA lentiviruses. The infected cells were then selected with 1 mg/L puromycin (Invivogen, San Diego, CA, USA) for 2 weeks to obtain cells with stable overexpression or

knockdown of SGO1-AS1. Two siRNAs targeting ZEB1 were designed and synthesized by Sangon Biotech (Shanghai, China), and their sequences are shown as follows: #1 sense, GGCAAGUGUUGGAGAAUAAUC, antisense, UUAUUCUCCAACACUUGCCUU; #2 sense, GGACAGCACAGUAAAUCUACA, antisense, UAGAUUUACUGUGCUGUCCUG. To construct the reporter vectors for SGO1-AS1 promoter activity, wild-type SGO1-AS1 promoter sequence (1kb of sequence upstream of the transcription start site) and its ZEB1-binding site mutated sequences were chemosynthesized in Huada (Shenzhen, Guangdong, China) and inserted into the vector pGL3 basic (Promega) upstream of the firefly luciferase gene.

PTBP1 knockout by CRISPR/Cas9

The small guide RNA (sgRNA) targeting the genome sequence of PTBP1 was cloned into LentiCRISPRv2 (Addgene), and lentivirus particles were generated by co-transfecting the recombinant vector and packaging plasmids into HEK293T packaging cells. MKN28 cells were infected with lentiviruses, and single cells were isolated 48 h after infection by FACS (BD FACS Aria III) into 96-well plates. Independent clones were allowed to grow for 3 weeks. PTBP1 knockout cells were identified by Western blotting and targeted Sanger sequencing. The sgRNA targeting PTBP1 was 5’-CAGAGCAGACCCGCGGGGGA-3’.

Western blotting analysis

Western blotting analysis was performed using the standard procedures. The following primary antibodies were used in the experiments: anti-PTBP1 antibody (Cell Signaling Technology, Beverly, MA, USA), anti-PTBP2 antibody (Abcam, Cambridge, UK), anti-PTBP3 antibody (Sigma-Aldrich, St. Louis, MO, USA), anti-HNRNPK antibody (Abcam), anti-HNRNPM antibody (Sigma-Aldrich), anti-FUBP3 antibody (Abcam), anti-CPSF2 antibody (Abcam), anti-G3BP2 antibody (Atlas Antibodies), anti-TGFβ1 antibody (Proteintech Group), anti-TGFβ2 antibody (Abcam), anti-p-SMAD2 antibody (Cell Signaling Technology), anti-SMAD2 antibody (Cell Signaling Technology), anti-p-SMAD3 antibody (Cell Signaling Technology), anti-SMAD3 antibody (Cell Signaling Technology), anti-SMAD5 antibody (Abcam), anti-ID2 antibody (Abcam), anti-ZEB1 antibody (Abcam), anti-SNAI antibody (Abcam), anti-E-cadherin antibody (Proteintech Group), anti-Vimentin antibody (Cell Signaling Technology), anti-N-cadherin antibody (Cell Signaling Technology) and anti-GAPDH antibody (Sigma-Aldrich). The blots were incubated with goat anti-rabbit or anti-mouse secondary antibody (Sigma-Aldrich) and visualized with a commercial ECL kit (Pierce, Rockford, IL).

RNA pull-down assay

RNA pull-down assays were carried out as previously described. Briefly, The SGO1-AS1 sequences were cloned into pMD20-T vector with T7 promoter and *in vitro* transcribed with biotin RNA labeling mix and T7 RNA polymerase (Invitrogen) according to the manufacturer’s instructions. The RNA pulldown assay was performed using the Pierce Magnetic RNA-Protein Pull-Down Kit (Millipore, Bedford, MA, USA) in accordance with the manufacturer’s instructions. Finally, the retrieved proteins were measured on sodium dodecyl sulfate-polyacrylamide gel electrophoresis (SDS PAGE) gels for mass spectrometry or Western blot analysis.

RNA immunoprecipitation (RIP) assay

RIP assay was performed using the Magna RIP RNA-Binding Protein Immunoprecipitation Kit (Millipore, Bedford, MA, USA) according to the manufacturer's instructions. Briefly, 100 μL cell extract was incubated with magnetic beads-antibody complex. The antibodies were used for RIP, and IgG served as a negative control. The precipitated RNAs were isolated using Trizol (Invitrogen) for RNA sequencing (RNA-seq) or qRT-PCR analyses.

Chromatin immunoprecipitation (ChIP) assay

ChIP assay was performed using a Chromatin Immunoprecipitation Assay Kit (Millipore, Bedford, MA, USA). MKN28 cells were exposed to TGFβ1 or vehicle for 24 h, then crosslinked, lysed and sonicated. Immunoprecipitation was performed using anti-ZEB1 antibody (Abcam, Cambridge, UK) and IgG. The precipitated DNA was quantified using qPCR and normalized by respective 2% input.

RNA-seq analysis

To seek out differentially expressed genes upon PTBP1 knockout, total RNA was isolated from PTBP1 knockout or control MKN28 cells using TRIZOL reagent, and PolyA RNA was subsequently purified from total RNA using NEBNext Poly(A) mRNA Magnetic Isolation Module. RNA-seq was performed to detect the mRNA expression profiles at GENTED (Shanghai, China) using HiSeq3000 (Illumina, USA). The differential genes were selected with fold change > 2 and a P-value < 0.05. To reveal PTBP1-bound mRNAs, RIP experiments were conducted using a PTBP1 antibody (Cell Signaling Technology) or IgG. Total RNA was isolated with Trizol (Invitrogen), and ribosomal RNA was removed from total RNA. RNA-seq was performed at CLOUDSEQ (Shanghai, China) using HiSeq3000 (Illumina, USA). Data are available via GEO under accession numbers GSE157582 and GSE157941.

Luciferase reporter assay

HEK293T cells were seeded in 24-well plates and transfected with the SGO1-AS1 promoter reporter constructs with wild-type or mutated ZEB1 binding sites. The pTK-Cluc vector was used as the internal transfection control. The transfected cells were treated with TGFβ1 (5 ng/mL) or vehicle control for 48 h, and Firefly and Renilla luciferase activities were measured using the Dual-Luciferase Reporter Assay System (Promega), following the manufacturer's instructions. SBE4 promoter luciferase reporter vector (Addgene) was transfected into PTBP1 knockout or control MKN28 cells. In addition, HEK293T cells were transfected with SBE4 promoter reporter vectors and then treated with conditioned medium from cells with SGO1-AS1 knockdown or overexpression. Firefly and Renilla luciferase activities were measured 48 h after transfection using the dual luciferase system.

Cell invasion, migration and proliferation assays

For the cell invasion assay, starved cells suspended in serum-free DMEM were seeded into the upper chamber with Matrigel in the insert of a 24-well culture plate (Corning Costar). Medium containing 15% fetal bovine serum was added to the lower compartment as a chemoattractant. After incubation for 48 h, the invasive cells adhering to the lower membrane of the inserts were fixed, stained, counted and imaged. Cell migration ability was measured using the wound-healing assay. Cells were placed into 6-well plates

and cultured until 90% confluence. An artificial scratch was created using a 10 μL pipette tip, and the cells were cultured in serum-free medium. Wound closure images were captured in the same field under magnification. Cell proliferation was examined using cell counting. Cells were seeded into 6-well plates, and the cell numbers were counted after 1, 2, 3, 4, 5, 6 and 7 days of culturing in DMEM supplemented with 10% fetal bovine serum using a Coulter Counter.

Sphere culture

Cells were seeded into ultra-low attachment 6-well plates (Corning Costar) and cultured in DMEM/F12 medium (Gibco) supplemented with 2% B27 (Life Technologies), 20 ng/ml FGF (R&D Systems, MN, USA), 20 ng/ml EGF (R&D Systems) and 5 μg/ml insulin (R&D Systems). Two weeks later, sphere pictures were taken and sphere formation ratios were calculated.

Animal experiments

Female 6- to 8-week-old BALB/c nude mice were purchased from the Experimental Animal Center of Guangdong (Foshan, Guangdong, China). To investigate the role of SGO1-AS1 in tumor metastasis and growth *in vivo*, luciferase-labeled SGC7901 cells overexpressing SGO1-AS1 or control vector were injected into the tail vein or stomach of the BALB/c nude mice. The luciferase signal intensity was monitored *in vivo* using an In Vivo Imaging System (FX PRO, Bruker, Billerica, MA, USA). Then, the mice were sacrificed, and the metastatic foci in the abdominal cavity and lung were evaluated. In addition, SGC7901 cells with SGO1-AS1 overexpression or control cells were subcutaneously injected into the nude mice. The mice were sacrificed after 28 days of implantation, and the tumors were excised and weighed.

To confirm the inhibitory effects of SGO1-AS1 on metastasis activity via TGFβ signaling *in vivo*, we orthotopically implanted luciferase-labeled MKN28 cells stably expressing shSGO1-AS1 or control shRNA into the stomach of nude mice and treated the mice with saline, SB431542 (20 mg/kg body weight, i.p) three times per week for 3 weeks. The luciferase signal intensity was monitored *in vivo* by bioluminescence imaging.

Statistical analysis

A Student's t-test or a chi-square test was used for two-sample comparisons. Differences among three or more groups were analyzed with two-way analysis of variance. The overall survival curves were plotted using the Kaplan-Meier method, and survival differences were evaluated with a log-rank test. Cox regression was utilized to estimate the hazard ratio and 95% confidence intervals for survival. Pairwise expression correlation was analyzed using Pearson correlation tests. Values of $P < 0.05$ were considered as statistically significant.

Results

SGO1-AS1 is downregulated in gastric carcinoma tissues and inversely associated with tumor progression

To identify GC-relevant lncRNAs, we examined lncRNA expression profiles in five paired GCs and adjacent normal mucosa tissues using a microarray. We found that 185 lncRNAs were differentially expressed in GCs compared to adjacent tissues (fold change > 2 and $P < 0.05$, Fig. 1a), 13 of which were upregulated or downregulated more than fourfold. We selected these lncRNAs with a more than fourfold differences for qPCR expression validation in a small GC cohort (18 pairs of GC and adjacent normal tissues, Cohort 1). Among these lncRNAs, SGO1-AS1 was the most differentially expressed in GC relative to normal samples (Additional file 1: Fig. S1). Furthermore, SGO1-AS1 was also downregulated in GC tissues from one publicly published dataset (GSE50710) [12] in GEO database (Fig. 1b).

The SGO1-AS1 gene has two annotated transcripts in the Genecode database (GENCODE V23, Additional file 1: Fig. S2a). Nevertheless, the expression of the short isoform was not detected in any GC cell lines, GC tissues, or normal samples in this study (data not shown), but the long isoform was expressed to varying degrees in GC tissues, normal samples and GC cell lines (Fig. 1c, and Additional file 1: Fig. S3a). We therefore focused on the long isoform SGO1-AS1 for our further analyses. For convenience, we here refer to this isoform as SGO1-AS1. In 5' and 3' RACE, SGO1-AS1 was revealed to be a 1392-nucleotide antisense transcript (Additional file 1: Fig. S2b), with a sequence that is partially complementary to SGO1 mRNAs. We examined the coding capability of SGO1-AS1 using the Coding-Potential Assessment Tool (CPAT) [13] and the Coding Potential Calculator (CPC) [14]. The results showed that SGO1-AS1 has no protein-coding potential (Additional file 1: Fig. S2c). Furthermore, SGO1-AS1 was mainly located in the cytoplasm of normal and GC cells, shown by qRT-PCR analysis with nuclear/cytoplasmic RNA fractionation (Additional file 1: Fig. S2d) and RNA ISH analysis (Fig. 1g).

In another cohort of 92 pairs of GC and adjacent normal tissues (Cohort 2), we further confirmed the downregulation of SGO1-AS1 in GC tissues via qRT-PCR analysis, and 63% (58/92) of the GC cases showed more than 2-fold downregulation of SGO1-AS1 relative to the corresponding normal tissues (Fig. 1c). Moreover, decreased levels of SGO1-AS1 were correlated with clinical stage, lymph node metastasis and distant metastasis (Fig. 1d-f). This result was also confirmed by ISH analyses of 80 cases of normal gastric mucosa tissues and 95 GC tumor tissues (Cohort 3) in tissue microarrays (Fig. 1g-i, and Additional file 1: Table S5). Moreover, survival analysis showed that low levels of SGO1-AS1 expression in GC tissues were associated with unfavorable overall survival for GC patients (log rank = 11.67, $P = 0.0006$, Fig. 1i). Simultaneously, Cox's proportional hazards regression analysis indicated that low SGO1-AS1 expression was an independent predictor for GC prognosis (Additional file 1: Table S6). Taken together, these results demonstrate a reverse correlation between SGO1-AS1 expression and GC progression.

SGO1-AS1 suppresses gastric carcinoma cell invasion and metastasis

Given that the inverse relationship between SGO1-AS1 expression level and GC progression, we evaluated whether SGO1-AS1 could affect GC cell invasion and metastasis. To address this, we first tested the endogenous expression levels of SGO1-AS1 in gastric cell lines and found it to be expressed at low levels

in SGC7901, BGC823 and MGC803 cells and at relatively high levels in MKN28 cells (Additional file 1: Fig. S3a). Therefore, the SGC7901 and BGC823 cell lines were selected to stably overexpress SGO1-AS1, and MKN28 was chosen to stably deplete it with effective shRNAs, using a lentiviral system (Additional file 1: Fig. S3b, c). The results from transwell and wound-healing assays showed that stable SGO1-AS1 overexpression repressed the migration and invasion of SGC7901 and BGC823 cells (Fig. 2a, c and Additional file 1: Fig. S3d). By contrast, knockdown of SGO1-AS1 by two different shRNAs significantly enhanced migration and invasion activities of MKN28 cells (Fig. 2b, d). Moreover, SGO1-AS1 inhibited long-term cell growth but had no significant impact on short-term growth (Additional file 1: Fig. S3e). In addition, soft-agar colony formation assays revealed that SGO1-AS1 overexpression markedly reduced colony number and size, while silencing it had the reverse effect (Additional file 1: Fig. S3f, g).

In our subsequent *in vivo* study, SGC7901 cells with stable expression of empty vector or SGO1-AS1 were injected into the tail-vein of nude mice and the formation of pulmonary metastases was measured. Overexpression of SGO1-AS1 reduced the ability of SGC7901 cells to form lung metastases in the mice (Fig. 2e). Moreover, the survival time of mice injected with SGC7901 cells was prolonged when SGO1-AS1 was overexpressed (Fig. 2f). In addition, SGC7901 cells with stable expression of SGO1-AS1 or empty vector were injected into the corpus of the stomach of nude mice. Lower metastasis signals were observed in the SGO1-AS1-overexpressing group than in the control group by bioluminescence imaging (Fig. 2g). Then, the mice were sacrificed, and the metastatic foci in the abdominal cavity were evaluated. We found that 90% (9/10) of the control mice had metastatic nodules in the liver, but only 40% of the mice in the SGO1-AS1-overexpressing group did (Fig. 2g). In addition, 70% (7/10) of the mice in the control group and only 20% (2/10) of the mice in the SGO1-AS1-overexpressing group had intestine and mesentery metastases (Fig. 2g). Subcutaneous xenografts were also established in nude mice using SGC7901 cells with stable expression of empty vector or SGO1-AS1. The overexpression of SGO1-AS1 moderately inhibited tumor growth (Additional file 1: Fig. S3h). Taken together, these findings demonstrate that SGO1-AS1 inhibits GC invasion and metastasis both *in vitro* and *in vivo*.

SGO1-AS1 is associated with PTBP1

We next explored the molecular mechanism underlying SGO1-AS1-induced inhibition of metastasis. SGO1-AS1 is an antisense transcript that partially overlaps the coding gene SGO1 (or SGOL1). We therefore examined whether SGO1-AS1 would affect the expression of the sense gene SGO1, and found that although knockdown of SGO1-AS1 moderately induced SGO1 expression, overexpression of SGO1-AS1 did not affect the expression of SGO1 (Additional file 1: Fig. S4a, b). We next identified potential SGO1-AS1-interacting proteins. We performed RNA pull-down assays *in vitro* with biotinylated SGO1-AS1, followed by SDS-PAGE electrophoresis, and an overtly differential band at approximately 60 kD in the sense lane was selected for mass spectrum analyses (Fig. 3a). Our results revealed several potential proteins that were pulled down with SGO1-AS1 RNA, and of these, PTBP1 received the highest score (Additional file 1: Table S7). Biotin-labeled RNA pulldown followed by Western blotting analysis confirmed PTBP1 and G3BP2 as SGO1-AS1-binding proteins (Fig. 3b). Furthermore, RIP followed by qRT-PCR assays

showed that the antibodies against either PTBP1 or G3BP2 could significantly enrich for SGO1-AS1 compared to controls (Fig. 3c).

PTBP1, a member of the heterogeneous nuclear ribonucleoprotein (hnRNP) family, is a critical regulator of mRNA splicing [15, 16], RNA stability [17], transportation [18], localization [19] and translation [20, 21]. PTBP1 has been shown to be involved in tumorigenesis, though its effects on malignancy appear to be cell-type dependent [16, 22, 23]. We focused on PTBP1 as an interacting partner of SGO1-AS1 for further investigation. To determine the binding region of SGO1-AS1 to PTBP1, we prepared a series of biotin-labeled SGO1-AS1 probes with deletion mutants and performed an *in vivo* RNA pull-down experiment with them. We found that the 1-415 nt fragment of SGO1-AS1 was sufficient to bind PTBP1 (Fig. 3d). Considering that PTBP1 binds to pyrimidine-rich sequences (UCUUC), we identified the accurate binding site of PTBP1 in SGO1-AS1 (258–319 nt) via RNA pulldown assays (Fig. 3e). PTBP1 contains four RRM domains for binding to RNA [24]. To investigate which domain of PTBP1 accounts for its interaction with SGO1-AS1, we performed RIP assays, using a series of Flag-tagged PTBP1 deletion mutants, and found that the RRM2 domain of PTBP1 had the strongest association with SGO1-AS1 (Fig. 3f).

SGO1-AS1 regulates TGFB1/2 mRNA stability via interaction with PTBP1

PTBP1 is an RNA-binding protein (RBP) known for its role in mRNA metabolism through binding to target mRNAs [20]. We hypothesized that the association between SGO1-AS1 and PTBP1 may influence the effects of PTBP1 on its target mRNAs. We generated a stable PTBP1-knockout MKN28 cell line using CRISPR-Cas9 technology (Fig. 4a, e) and performed RNA-seq analysis. A comparison of PTBP1-knockout to control cells revealed that 393 mRNAs were upregulated and 348 mRNAs were downregulated (Fig. 4b). Kyoto Encyclopedia of Genes and Genomes (KEGG) analysis revealed that the downregulated genes were apparently enriched in TGFβ signaling and pathways regulating stem cells, extracellular matrix (ECM) and focal adhesion (Fig. 4c). The downregulated genes involved in the TGFβ pathway in PTBP1-knockout MKN28 cells were further validated at the mRNA and protein levels (Fig. 4d, e). The similar result was observed in SGC7901 cells transfected with PTBP1 shRNA (Additional file 1: Fig. S5A). Interestingly, based on SGO1-AS1 levels, we performed gene set enrichment analysis (GSEA) using the cancer genome atlas (TCGA: https://cancergenome.nih.gov) stomach adenocarcinoma RNA-seq dataset demonstrated that TGFβ1 target genes were significantly enriched in GC patients with low SGO1-AS1 expression (Fig. 4f), implying a role of this lncRNA in regulating TGFβ signaling.

Given that PTBP1 is an RNA binding protein [20]. we performed RIP-seq experiment using anti-PTBP1 antibody or rabbit immunoglobulin G to reveal PTBP1 bound RNAs. We identified 5186 transcripts potentially bound by PTBP1 and 173 transcripts that overlapped between PTBP1-bound mRNAs and differentially expressed genes following PTBP1 knockout, three of which (TGFB1, TGFB2 and ID2) are related to the TGFβ pathway (Fig. 4g). PTBP1 interaction with TGFB1, TGFB2 or ID2 mRNA was further confirmed by RIP followed by qPCR (Fig. 4h and Additional file 1: Fig. S5b). Importantly, SGO1-AS1 overexpression resulted in a much increase in SGO1-AS1 association with PTBP1, while the TGFB1/2

mRNA binding of PTBP1 was markedly decreased in SGC7901 cells (Fig. 4i). Conversely, the association of TGFB1/2 mRNA with PTBP1 was increased upon knockdown of SGO1-AS1 in MKN28 cells (Fig. 4j). However, the regulation of SGO1-AS1 expression did not influence the association between the PTBP1 protein and ID2 mRNA (Additional file 1: Fig. S5c). Furthermore, we found that TGFB1/2 mRNA was mainly bound to the RRM2 domain of PTBP1 (Additional file 1: Fig. S5d), the region bound by SGO1-AS1 (Fig. 3f). Together, these results suggest that SGO1-AS1 competes with TGFB1/2 mRNA to bind to PTBP1.

Since our above results indicate that depletion of PTBP1 reduces the TGFB mRNA level, we asked whether PTBP1 and SGO1-AS1 may influence TGFB mRNA stability. Actinomycin D (ACD) was used to block de novo transcription in PTBP1-knockout and control cells that were infected with SGO1-AS1 shRNA. As expected, the depletion of PTBP1 increased TGFB mRNA degradation following ACD treatment in MKN28 cells. However, silencing SGO1-AS1 stabilized TGFB mRNAs, while having no significant effect on TGFB mRNA stability under conditions in which PTBP1 was depleted (Fig. 4k). Furthermore, the forced expression of SGO1-AS1 facilitated TGFB1/2 mRNA degradation, and the co-overexpression of PTBP1 abrogated this effect, although the overexpression of PTBP1 alone failed to influence TGFB mRNA stability (Fig. 4l), indicating that PTBP1 is necessary for SGO1-AS1-mediated TGFB mRNA decay. Consistent with this, knockdown of SGO1-AS1 increased TGFβ1/2 proteins, which was offset upon PTBP1 knockout (Fig. 4m). Conversely, SGO1-AS1 overexpression remarkably downregulated TGFβ protein expression, and this downregulation was reversed by the co-expression of PTBP1 (Fig. 4m). Moreover, the xenograft tumors generated by SGO1-AS1-overexpressing SGC7901 cells featured lower TGFB1/2 expression than control tumors (Additional file 1: Fig. S5e, f). Overall, the results demonstrate that SGO1-AS1 inhibits TGFB1/2 mRNA expression via a PTBP1-mediated mechanism.

SGO1-AS1 impedes TGFβ signaling, EMT and stemness

As SGO1-AS1 reduces TGFβ production, we evaluated whether SGO1-AS1 may affect TGFβ downstream signaling. As expected, silencing SGO1-AS1 enhanced the phosphorylation of SMADs and induced the transcriptional activity of SBE4 (SMAD-binding element) in control cells but showed little effect in PTBP1-deficient cells, and the activation of TGFβ signaling by SGO1-AS1 knockdown was reversed by treatment with TGFβ type I receptor (TβRI) inhibitor SB431542 (Fig. 5a, b). These results indicate that SGO1-AS1 acts as a potent antagonist of TGFβ/SMAD signaling in a PTBP1-dependent manner.

TGFβ is a major inducer of EMT and stimulates stemness, invasion and metastasis in cancer cells [25, 26]. Therefore, we examined whether silencing SGO1-AS1 could promote the ability of GC cells to undergo EMT. As shown in Fig. 5c and Additional file 1: Fig. S6a, knockdown of SGO1-AS1 in MKN28 cells reduces epithelial features but increases mesenchymal ones, as evidenced by the reduced expression of the epithelial marker (E-cadherin) but the increased levels of mesenchymal markers (Vimentin and N-cadherin), as well as the elongation of cell bodies. We also examined the levels of EMT-inducing transcription factors (EMT-TFs) ZEB1, ZEB2, TWIST1, SNAI and SLUG, and showed that the expression levels of ZEB1, SNAI and SLUG were increased upon SGO1-AS1 knockdown (Fig. 5e). Moreover, SGO1-AS1 knockdown induced mesenchymal-like features were reversed by PTBP1 knockout or SB431542

treatment (Fig. 5c, e and Additional file 1: Fig. S6a). By contrast, SGO1-AS1 overexpression in SGC7901 cells dampened the EMT process, which was rescued by the treatment of the recombinant TGFβ1 protein (Fig. 5d, e and Additional file 1: Fig. S6a). Consistently, the invasive activity was significantly decreased in SGO1-AS1-deleted MKN28 cells upon PTBP1 loss or SB431542 treatment, but it was rescued in SGO1-AS1-overexpressed SGC7901 cells with the addition of recombinant TGFβ1(Fig. 5f and Additional file 1: Fig. S6b). To confirm the inhibitory effects of SGO1-AS1 on metastatic activity through TGFβ signaling *in vivo*, we orthotopically implanted SGO1-AS1 knockdown cells into the nude mice and treated them with SB431542 (three times per week). Consistent with the overexpression study (Fig. 2g), higher metastasis signals were found in the SGO1-AS1 knockdown group compared to the signals in the control group, while SB431542 treatment exhibited a significant reduction of metastases in mice harboring SGO1-AS1 knockdown cells (Fig. 5i).

We then examined the effects of SGO1-AS1 on stemness. SGO1-AS1 knockdown increased the tumor spheroid formation and ALDH1 + population, whereas loss of PTBP1 or treatment with SB431542 significantly abolished these effects (Fig. 5g, h and Additional file 1: Fig. S6c). Conversely, SGO1-AS1 overexpression reduced the stemness features in SGC7901 cells and the addition of TGFβ1 induced the stemness features in SGO1-AS1-overexpressing cells. Collectively, these data indicated that SGO1-AS1 attenuates EMT, stemness and metastasis via PTBP1-mediated TGFβ signaling.

SGO1-AS1 reduces TGFβ autocrine

Because our results showed that SGO1-AS1 reduced TGFβ expression and its downstream signaling, we reasoned that SGO1-AS1 might influence the secretion of these cytokines to interrupt the tumor microenvironment. Indeed, SGO1-AS1 knockdown induced but SGO1-AS1 overexpression inhibited the secretion of these cytokines, as observed through enzyme linked immunosorbent assay (ELISA) (Fig. 6a, b). To confirm that SGO1-AS1 modulates TGFβ autocrine signaling, we collected conditioned medium from SGO1-AS1-knockdown MKN28 cells or SGO1-AS1-overexpressing SGC7901 cells, transferred the conditioned medium to HEK293T cells and performed SBE4 transcription assays. The results showed that the conditioned medium collected from SGO1-AS1-silencing cells activated SBE4 transcription (Fig. 6c). By contrast, SBE4 transcription was downregulated in HEK293T cells with administration of the conditioned medium collected from SGO1-AS1-overexpressing cells compared to that collected from the control cells. We next explored the invasive phenotype of GC cells incubated with conditioned medium. As expected, MKN28 cells incubated with conditioned medium collected from SGO1-AS1-silencing MKN28 cells exhibited higher capacities of migration and invasion than cells incubated with conditioned medium collected from control cells, whereas SGC7901 cells incubated with conditioned medium collected from SGO1-AS1-overexpressing SGC7901 cells had reduced migration and invasion abilities compared to cells incubated with conditioned medium collected from control SGC7901 cells (Fig. 6d, e). These data indicate that SGO1-AS1 reduces the autocrine of TGFβ cytokines.

TGFβ represses SGO1-AS1 transcription via ZEB1

Having found that SGO1-AS1 antagonizes TGFβ signaling via promoting TGFB mRNA degradation, we next investigated the response of SGO1-AS1 to TGFβ. We treated SGC7901 cells with TGFβ1 and found that SGO1-AS1 expression was inhibited but the well-known TGFβ targets (SNAI, ZEB1) [27, 28] were induced in a dose-dependent manner (Fig. 7a). SGO1-AS1 downregulation by TGFβ treatment was confirmed in two other GC cell lines (Fig. 7b). We next exposed the cells to the TGFβRI inhibitor SB431542 and found that SB431542 treatment induced SGO1-AS1 expression, accompanied by the downregulation of SNAI and ZEB1 (Fig. 7c). We carried out bioinformatics analysis using JASPAR (http://jaspar.genereg.net/) to identify potential regulatory transcription factors. Bioinformatics analysis revealed four ZEB1 binding motifs at -222 to -214 (site A), -731 to -721 (site B), -822 to -814 (site C) and −947 to -940 (site D) inside the SGO1-AS1 promoter (Fig. 7d, e). ZEB1 is a downstream target gene of TGFβ and has been reported to be a master regulator of EMT and cancer metastasis [29]. We evaluated whether the downregulation effects of TGFβ on SGO1-AS1 occur via ZEB1. A luciferase reporter assay showed that luciferase activity for reporter constructs containing 1 kb of wild-type SGO1-AS1 promoter fell by approximately 2-fold in TGFβ-treated cells relative to control cells, and the ZEB1 binding site mutation on SGO1-AS1 promoter abolished this effect (Fig. 7f). We then knocked down ZEB1 in GC cells with TGFβ1 treatment to study its effects on SGO1-AS1 levels and found that depletion of ZEB1 completely reversed the repressive effects of TGFβ1 on SGO1-AS1 expression (Fig. 7g). Using ChIP, we discovered significant enrichment in the binding of ZEB1 to the promoter region of SGO1-AS1 in cells with TGFβ1 treatment relative to control cells (Fig. 7h). Taken together, our data indicate that TGFβ downregulates SGO1-AS1 through inducing ZEB1.

SGO1-AS1 downregulation correlates with high expression of TGFB1/2 and ZEB1 in gastric carcinoma specimens

We sought to verify whether our findings could be extended to patients with gastric carcinoma. The expression levels of TGFB1, TGFB2 and ZEB1 were detected by qRT-PCR in 92 pairs of gastric carcinoma specimens and adjacent normal tissues (Cohort 2). The expression levels of these three genes were significantly increased in tumors when compared to those in normal tissues, and 51.1% (47/92), 58.7% (54/92) and 39.1% (36/92) of the GC samples showed more than 2-fold upregulation of TGFB1, TGFB2 and ZEB1, respectively (Fig. 8a-c). Moreover, high levels of TGFB1/2 and ZEB1 were significantly associated with lymphatic invasion and advanced tumor stage (Fig. 8d-f). GCs with metastasis expressed higher levels of TGFB1/2 and ZEB1 than those without metastasis (Fig. 8d-f). Importantly, TGFB1/2 and ZEB1 were inversely correlated with SGO1-AS1, whereas TGFB1/2 was positively associated with ZEB1 in GC tissues (Fig. 8g), further confirming the SGO1-AS1-TGFB-ZEB1 regulatory axis in GC. We also observed that TGFB1 had no significant association with TGFB2 expression (Fig. 8g).

Discussion

Most patients with GC die from metastatic disease, but little is known about the mechanisms of metastasis in gastric tumors [2]. In this study, we identified a metastasis-suppressive lncRNA, SGO1-AS1,

which is decreased in progressed gastric cancer and reversely correlates with gastric tumor metastasis. We further revealed that SGO1-AS1 interacts with the protein PTBP1, and their interaction competitively reduces TGFB1/2 mRNA binding to PTBP1. Then, the decreased binding of TGFB1/2 mRNA to PTBP1 leads to the reduction of TGFB1/2 mRNA stability and the reduced TGFβ production, thus preventing EMT and metastasis. In addition, TGFβ in turn represses SGO1-AS1 transcription via inducing ZEB1. Thus, SGO1-AS1 and TGFβ form a double-negative feedback loop via ZEB1 to regulate EMT and metastasis (Fig. 8h).

LncRNAs often exert their functions through the proteins they interact with [30]. Here, we identified PTBP1 as an SGO1-AS1-interacting protein. PTBP1 has been shown to be involved in tumorigenesis by regulating alternative splicing [31, 32], controlling mRNA stability [17, 33] and determining mRNA localization [19]. For example, PTBP1 enhances PKM2 isoform and reduces PKM1 isoform by controlling PKM alternative splicing, which promotes aerobic glycolysis and provides a selective advantage for tumor formation [16, 34]. PTBP1 mediates MCL1 mRNA stability and regulates cellular apoptosis induced by antitubulin chemotherapeutics [23]. Of note, several lncRNAs have been reported to be associated with PTBP1 [17, 35, 36]. Hypoxia-induced lncRNA LUCAT1 interacts with PTBP1 in CRC cells, facilitating the association of a set of DNA damage related genes with PTBP1, and resulting in altered alternative splicing of these genes and conferring resistance to chemotherapeutic drugs in CRC cells [37]. LncRNA MEG3 can recruit PTBP1 to regulate small heterodimer partner mRNA stability and cholestatic liver injury [17]. Recruiting PTBP1 to target mRNAs appears to be a common mechanism among these lncRNAs. However, we found SGO1-AS1 interaction with PTBP1 reduces enrichment of this protein in TGFB1/2 mRNA to facilitate their decay. In addition to PTBP1, it is possible that SGO1-AS1 might bind to other proteins, such as G3BP2, to regulate GC metastasis, as G3BP2 was found to be a SGO1-AS1-interacting protein through mass spectrum analyses and verification analyses in our study. This and other proteins bound by SGO1-AS1 deserve further investigation in gastric carcinoma.

Identifying TGFβ-induced ZEB1 as a potent transcriptional repressor for SGO1-AS1 is another important finding of this study. Here, we demonstrated a reciprocal negative feedback loop between SGO1-AS1 and TGFβ/ZEB1. Although the well-documented double positive feedback loop between TGFβ and lncRNA [38–40], to the best of our knowledge, a reciprocal repressive loop between TGFβ and lncRNA have hardly been observed. Our current study provided evidence of a reciprocal repressive loop between TGFβ and lncRNA SGO1-AS1 in GC metastasis, where we showed that ZEB1 induced by TGFβ transcriptionally inhibits SGO1-AS1 expression; in turn, SGO1-AS1 inhibits TGFβ expression through the reduction of TGFB mRNA stability, which mediates the reciprocal repressive loop between TGFβ/ZEB1 and SGO1-AS1 in GC.

TGFβ signaling is highly conserved in multicellular organisms, involved in multiple cellular processes, such as cell growth, stemness, migration and invasion, EMT, ECM, remodeling and immune regulation [41]. The activation of canonical TGFβ signaling is caused by the binding of TGFβ ligands (TGFβ1, TGFβ2 and TGFβ3) to heteromeric TGFβ type I and II receptors, which phosphorylate SMAD2 and SMAD3, resulting in a complex formation with SMAD4 and nuclear translocation to regulate target gene transcription [42]. TGFβ has a critical role in tumorigenesis and tumor progression in a complex and

pleiotropic manner; in early tumor initiation, it plays a tumor-suppressive role by inhibiting cell proliferation and stimulating apoptosis; however, in advanced tumors, it promotes tumor progression via the induction of EMT, which correlates with increased invasiveness, metastasis and chemoresistance in tumor cells [43, 44]. Because of its role in advanced tumors, TGFβ is considered a therapeutic target. Several strategies have been proposed to inhibit TGFβ signaling to combat malignant tumors (e.g., small-molecule inhibitors of receptor kinases, TGFβ neutralizing antibodies and antisense compounds) [45]. Our finding that SGO1-AS1 and TGFβ/ZEB1 form a double-negative feedback loop hints at the possibility of new therapeutic approaches to block the TGFβ signal by introducing SGO1-AS1 or using the interference of ZEB1, although this remains to be confirmed by future studies.

Conclusions

Our study identified a metastasis-suppressive lncRNA that functions as an endogenous inhibitor of the TGFβ pathway and suppresses GC metastasis and progression. Our data further elucidate the importance of the double-negative feedback loop between SGO1-AS1 and TGFβ/ZEB1 in GC metastasis. These findings provide novel information for understanding the mechanisms underlying pathogenesis in GC metastasis, and new insight into the potential use of SGO1-AS1-TGFβ-ZEB1 for the development of new treatment strategies for GC.

Abbreviations

lncRNAs
long noncoding RNAs; GC:gastric carcinoma; qRT-PCR:quantitative reverse transcription polymerase chain reaction; ISH:in situ hybridization; EMT:epithelial-to-mesenchymal transition; GEO:gene expression omnibus; qPCR:quantitative polymerase chain reaction; RACE:rapid amplification of cDNA ends; DMEM:dulbecco's modified eagle's medium; shRNA:short hairpin RNA; sgRNA:small guide RNA; SDS-PAGE:sodium dodecyl sulfate-polyacrylamide gel electrophoresis; RIP:RNA immunoprecipitation; RNA-seq:RNA sequencing; ChIP:chromatin immunoprecipitation; NC:normal control; SD:standard deviation; CPAT:coding-potential assessment tool; CPC:coding potential calculator; hnRNP:heterogeneous nuclear ribonucleoprotein; RBP:RNA-binding protein; KO:knockout; KEGG:Kyoto Encyclopedia of Genes and Genomes; ECM:extracellular matrix; GSEA:gene set enrichment analysis; TCGA:the cancer genome atlas; ACD:actinomycin D; TβRI:TGFβ type I receptor; EMT-TFs:EMT-inducing transcription factors; ELISA:enzyme linked immunosorbent assay; WT:wild-type.

Declarations

Acknowledgments

Not applicable.

Authors' contributions

DH, KZ and MD designed the study. MD, YG and JX supervised the study. DH, KZ, YG, WZ, RZ and YX performed the experiments. JC, DH and YL conducted bioinformatics analysis and experiment data analyses. ND collected tissue specimens and clinical data. MD and JX wrote the manuscript. All authors read and approved the final manuscript.

Funding

This work was supported by the National Natural Science Foundation of China (No. 81972771, No. 81672452 and No. 81472625), National Natural Science Foundation of Guangdong Province (No. 2018B0303110015 and No. 2018A0303130314) and Guangdong Medical Research Foundation (No. B2018283).

Availability of data and materials

The microarray data have been deposited in the GEO data base under accession numbers GSE157289, GSE157582 and GSE157941.

Ethics approval and consent to participate

All the procedures carried out in the research involving human participants are in accordance with the ethical standards of the Institutional Review Board of Affiliated Cancer Hospital of Guangzhou Medical University. Each participant signed an informed consent before participating to this study. All animal studies were approved by the Institutional Animal Care and Use Committee of Guangzhou Medical University, and all animals were ethically and humanely treated.

Consent for publication

All authors agreed on the manuscript.

Competing interests

The authors declare no conflict of interest.

References

1. Sung H, Ferlay J, Siegel RL, Laversanne M, Soerjomataram I, Jemal A, et al. Global cancer statistics 2020: GLOBOCAN estimates of incidence and mortality worldwide for 36 cancers in 185 countries. CA Cancer J Clin. 2021.
2. Bernards N, Creemers GJ, Nieuwenhuijzen GA, Bosscha K, Pruijt JF, Lemmens VE. No improvement in median survival for patients with metastatic gastric cancer despite increased use of chemotherapy. Ann Oncol. 2013;24(12):3056-60.
3. Ponting CP, Oliver PL, Reik W. Evolution and functions of long noncoding RNAs. Cell. 2009;136(4):629-41.

4. Derrien T, Guigo R, Johnson R. The Long Non-Coding RNAs: A New (P)layer in the "Dark Matter". Front Genet. 2012;2:107.
5. Kopp F, Mendell JT. Functional Classification and Experimental Dissection of Long Noncoding RNAs. Cell. 2018;172(3):393-407.
6. Schonrock N, Harvey RP, Mattick JS. Long noncoding RNAs in cardiac development and pathophysiology. Circ Res. 2012;111(10):1349-62.
7. Liu HT, Liu S, Liu L, Ma RR, Gao P. EGR1-Mediated Transcription of lncRNA-HNF1A-AS1 Promotes Cell-Cycle Progression in Gastric Cancer. Cancer Res. 2018;78(20):5877-90.
8. Xu MD, Wang Y, Weng W, Wei P, Qi P, Zhang Q, et al. A Positive Feedback Loop of lncRNA-PVT1 and FOXM1 Facilitates Gastric Cancer Growth and Invasion. Clin Cancer Res. 2017;23(8):2071-80.
9. Sun TT, He J, Liang Q, Ren LL, Yan TT, Yu TC, et al. LncRNA GClnc1 Promotes Gastric Carcinogenesis and May Act as a Modular Scaffold of WDR5 and KAT2A Complexes to Specify the Histone Modification Pattern. Cancer Discov. 2016;6(7):784-801.
10. Zhuo W, Liu Y, Li S, Guo D, Sun Q, Jin J, et al. Long Noncoding RNA GMAN, Up-regulated in Gastric Cancer Tissues, Is Associated With Metastasis in Patients and Promotes Translation of Ephrin A1 by Competitively Binding GMAN-AS. Gastroenterology. 2019;156(3):676-91.e11.
11. He W, Liang B, Wang C, Li S, Zhao Y, Huang Q, et al. MSC-regulated lncRNA MACC1-AS1 promotes stemness and chemoresistance through fatty acid oxidation in gastric cancer. Oncogene. 2019;38(23):4637-54.
12. Hu Y, Wang J, Qian J, Kong X, Tang J, Wang Y, et al. Long noncoding RNA GAPLINC regulates CD44-dependent cell invasiveness and associates with poor prognosis of gastric cancer. Cancer Res. 2014;74(23):6890-902.
13. Wang L, Park HJ, Dasari S, Wang S, Kocher JP, Li W. CPAT: Coding-Potential Assessment Tool using an alignment-free logistic regression model. Nucleic Acids Res. 2013;41(6):e74.
14. Kong L, Zhang Y, Ye ZQ, Liu XQ, Zhao SQ, Wei L, et al. CPC: assess the protein-coding potential of transcripts using sequence features and support vector machine. Nucleic Acids Res. 2007;35:W345-9.
15. Vuong JK, Lin CH, Zhang M, Chen L, Black DL, Zheng S. PTBP1 and PTBP2 Serve Both Specific and Redundant Functions in Neuronal Pre-mRNA Splicing. Cell Rep. 2016;17(10):2766-75.
16. Calabretta S, Bielli P, Passacantilli I, Pilozzi E, Fendrich V, Capurso G, et al. Modulation of PKM alternative splicing by PTBP1 promotes gemcitabine resistance in pancreatic cancer cells. Oncogene. 2016;35(16):2031-9.
17. Zhang L, Yang Z, Trottier J, Barbier O, Wang L. Long noncoding RNA MEG3 induces cholestatic liver injury by interaction with PTBP1 to facilitate shp mRNA decay. Hepatology. 2017;65(2):604-15.
18. Monzon-Casanova E, Screen M, Diaz-Munoz MD, Coulson RMR, Bell SE, Lamers G, et al. The RNA-binding protein PTBP1 is necessary for B cell selection in germinal centers. Nat Immunol. 2018;19(3):267-78.

19. Matus-Nicodemos R, Vavassori S, Castro-Faix M, Valentin-Acevedo A, Singh K, Marcelli V, et al. Polypyrimidine tract-binding protein is critical for the turnover and subcellular distribution of CD40 ligand mRNA in CD4+ T cells. J Immunol. 2011;186(4):2164-71.
20. Sawicka K, Bushell M, Spriggs KA, Willis AE. Polypyrimidine-tract-binding protein: a multifunctional RNA-binding protein. Biochem Soc Trans. 2008;36(Pt 4):641-7.
21. Sun YM, Wang WT, Zeng ZC, Chen TQ, Han C, Pan Q, et al. circMYBL2, a circRNA from MYBL2, regulates FLT3 translation by recruiting PTBP1 to promote FLT3-ITD AML progression. Blood. 2019;134(18):1533-46.
22. Bielli P, Panzeri V, Lattanzio R, Mutascio S, Pieraccioli M, Volpe E, et al. The Splicing Factor PTBP1 Promotes Expression of Oncogenic Splice Variants and Predicts Poor Prognosis in Patients with Non-muscle-Invasive Bladder Cancer. Clin Cancer Res. 2018;24(21):5422-32.
23. Cui J, Placzek WJ. PTBP1 modulation of MCL1 expression regulates cellular apoptosis induced by antitubulin chemotherapeutics. Cell Death Differ. 2016;23(10):1681-90.
24. Pina JM, Reynaga JM, Truong AAM, Keppetipola NM. Post-Translational Modifications in Polypyrimidine Tract Binding Proteins PTBP1 and PTBP2. Biochemistry. 2018;57(26):3873-82.
25. Chiang SP, Cabrera RM, Segall JE. Tumor cell intravasation. Am J Physiol Cell Physiol. 2016;311(1):C1-C14.
26. Welm AL. TGFbeta primes breast tumor cells for metastasis. Cell. 2008;133(1):27-8.
27. Yuan JH, Yang F, Wang F, Ma JZ, Guo YJ, Tao QF, et al. A long noncoding RNA activated by TGF-beta promotes the invasion-metastasis cascade in hepatocellular carcinoma. Cancer Cell. 2014;25(5):666-81.
28. Larsen JE, Nathan V, Osborne JK, Farrow RK, Deb D, Sullivan JP, et al. ZEB1 drives epithelial-to-mesenchymal transition in lung cancer. J Clin Invest. 2016;126(9):3219-35.
29. Wu HT, Zhong HT, Li GW, Shen JX, Ye QQ, Zhang ML, et al. Oncogenic functions of the EMT-related transcription factor ZEB1 in breast cancer. J Transl Med. 2020;18(1):51.
30. Bhan A, Soleimani M, Mandal SS. Long Noncoding RNA and Cancer: A New Paradigm. Cancer Res. 2017;77(15):3965-81.
31. Xie R, Chen X, Chen Z, Huang M, Dong W, Gu P, et al. Polypyrimidine tract binding protein 1 promotes lymphatic metastasis and proliferation of bladder cancer via alternative splicing of MEIS2 and PKM. Cancer Lett. 2019;449:31-44.
32. Georgilis A, Klotz S, Hanley CJ, Herranz N, Weirich B, Morancho B, et al. PTBP1-Mediated Alternative Splicing Regulates the Inflammatory Secretome and the Pro-tumorigenic Effects of Senescent Cells. Cancer Cell. 2018;34(1):85-102.e9.
33. Liu C, Yang Z, Wu J, Zhang L, Lee S, Shin DJ, et al. Long noncoding RNA H19 interacts with polypyrimidine tract-binding protein 1 to reprogram hepatic lipid homeostasis. Hepatology. 2018;67(5):1768-83.

34. Jiang J, Chen X, Liu H, Shao J, Xie R, Gu P, et al. Polypyrimidine Tract-Binding Protein 1 promotes proliferation, migration and invasion in clear-cell renal cell carcinoma by regulating alternative splicing of PKM. Am J Cancer Res. 2017;7(2):245-59.
35. Ramos AD, Andersen RE, Liu SJ, Nowakowski TJ, Hong SJ, Gertz C, et al. The long noncoding RNA Pnky regulates neuronal differentiation of embryonic and postnatal neural stem cells. Cell Stem Cell. 2015;16(4):439-47.
36. Liu J, Li Y, Tong J, Gao J, Guo Q, Zhang L, et al. Long non-coding RNA-dependent mechanism to regulate heme biosynthesis and erythrocyte development. Nat Commun. 2018;9(1):4386.
37. Huan L, Guo T, Wu Y, Xu L, Huang S, Xu Y, et al. Hypoxia induced LUCAT1/PTBP1 axis modulates cancer cell viability and chemotherapy response. Mol Cancer. 2020;19(1):11.
38. Sakai S, Ohhata T, Kitagawa K, Uchida C, Aoshima T, Niida H, et al. Long Noncoding RNA ELIT-1 Acts as a Smad3 Cofactor to Facilitate TGFbeta/Smad Signaling and Promote Epithelial-Mesenchymal Transition. Cancer Res. 2019;79(11):2821-38.
39. Zhang K, Han X, Zhang Z, Zheng L, Hu Z, Yao Q, et al. The liver-enriched lnc-LFAR1 promotes liver fibrosis by activating TGFbeta and Notch pathways. Nat Commun. 2017;8(1):144.
40. Lang C, Dai Y, Wu Z, Yang Q, He S, Zhang X, et al. SMAD3/SP1 complex-mediated constitutive active loop between lncRNA PCAT7 and TGF-beta signaling promotes prostate cancer bone metastasis. Mol Oncol. 2020;14(4):808-28.
41. Derynck R, Zhang YE. Smad-dependent and Smad-independent pathways in TGF-beta family signalling. Nature. 2003;425(6958):577-84.
42. Shi Y, Massague J. Mechanisms of TGF-beta signaling from cell membrane to the nucleus. Cell. 2003;113(6):685-700.
43. Roberts AB, Wakefield LM. The two faces of transforming growth factor beta in carcinogenesis. Proc Natl Acad Sci U S A. 2003;100(15):8621-3.
44. Massague J. TGFbeta in Cancer. Cell. 2008;134(2):215-30.
45. Akhurst RJ, Hata A. Targeting the TGFbeta signalling pathway in disease. Nat Rev Drug Discov. 2012;11(10):790-811.

Figures

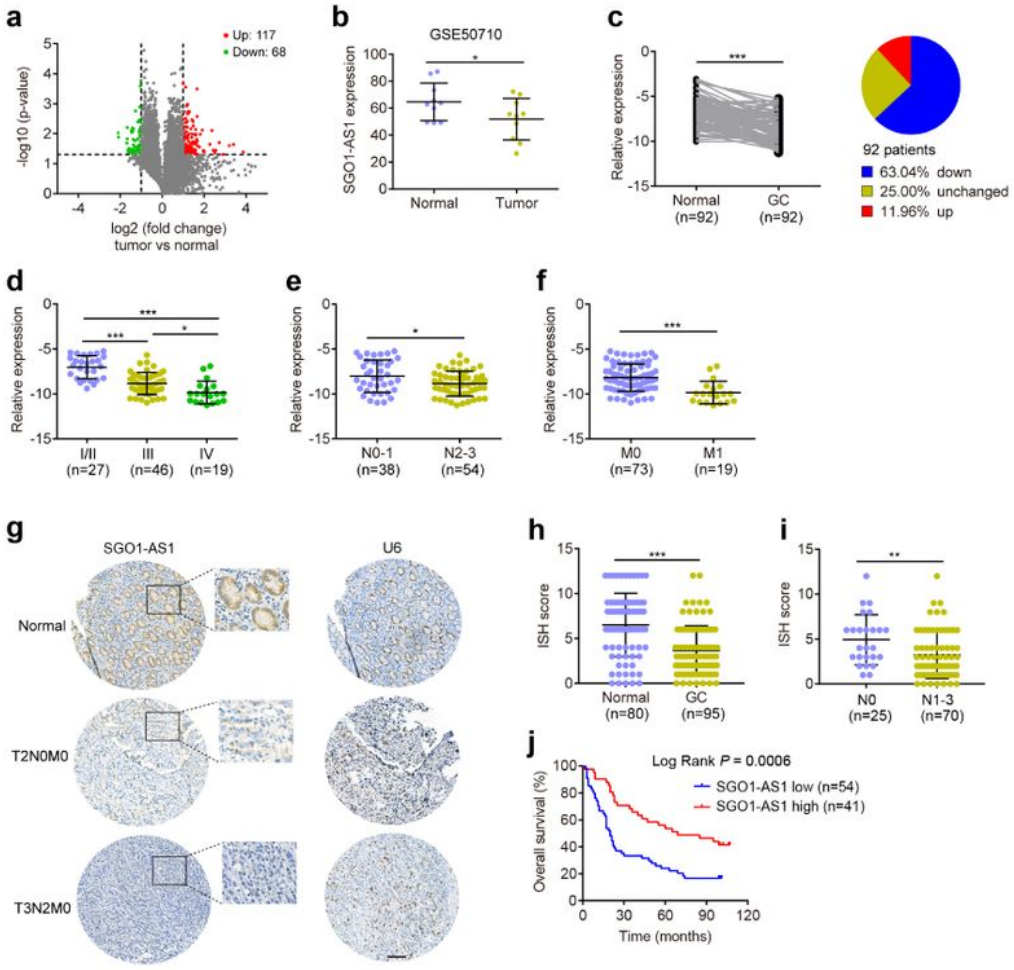

Figure 1

SGO1-AS1 is downregulated in GC tissues and associated with GC progression. a. Volcano plots of differentially expressed lncRNAs in GCs vs. matched normal tissues, shown in green and red, respectively. b. SGO1-AS1 expression levels in 10 pairs of GCs and adjacent normal tissues from the GEO dataset (GSE50710). c. Relative expression levels of SGO1-AS1 in 92 paired GCs and normal tissues from Cohort 2 patients were quantified by qRT-PCR. SGO1-AS1 was downregulated (>2-fold) in 63% (58 of 92) of the

GC tissues (tumor) relative to that in the adjacent noncancerous tissues (normal). d-f. Assessment of SGO1-AS1 expression levels in GCs according to their clinical stage (d) and status of lymph node (e) or distant metastasis (f) based on qPCR analysis in GC. g-i. RNA ISH analyses of SGO1-AS1 expression in 95 GC specimens and 80 normal tissues on tissue microarrays. Scale bar: 50 μm. j. Kaplan-Meier analyses of overall survival for patients with GCs (n = 95) based on SGO1-AS1 expression levels. The defined high and low expression levels of SGO1-AS1 were stratified according to the median expression level. Error bars indicate standard deviation (SD). *P < 0.05, **P < 0.01, ***P < 0.001.

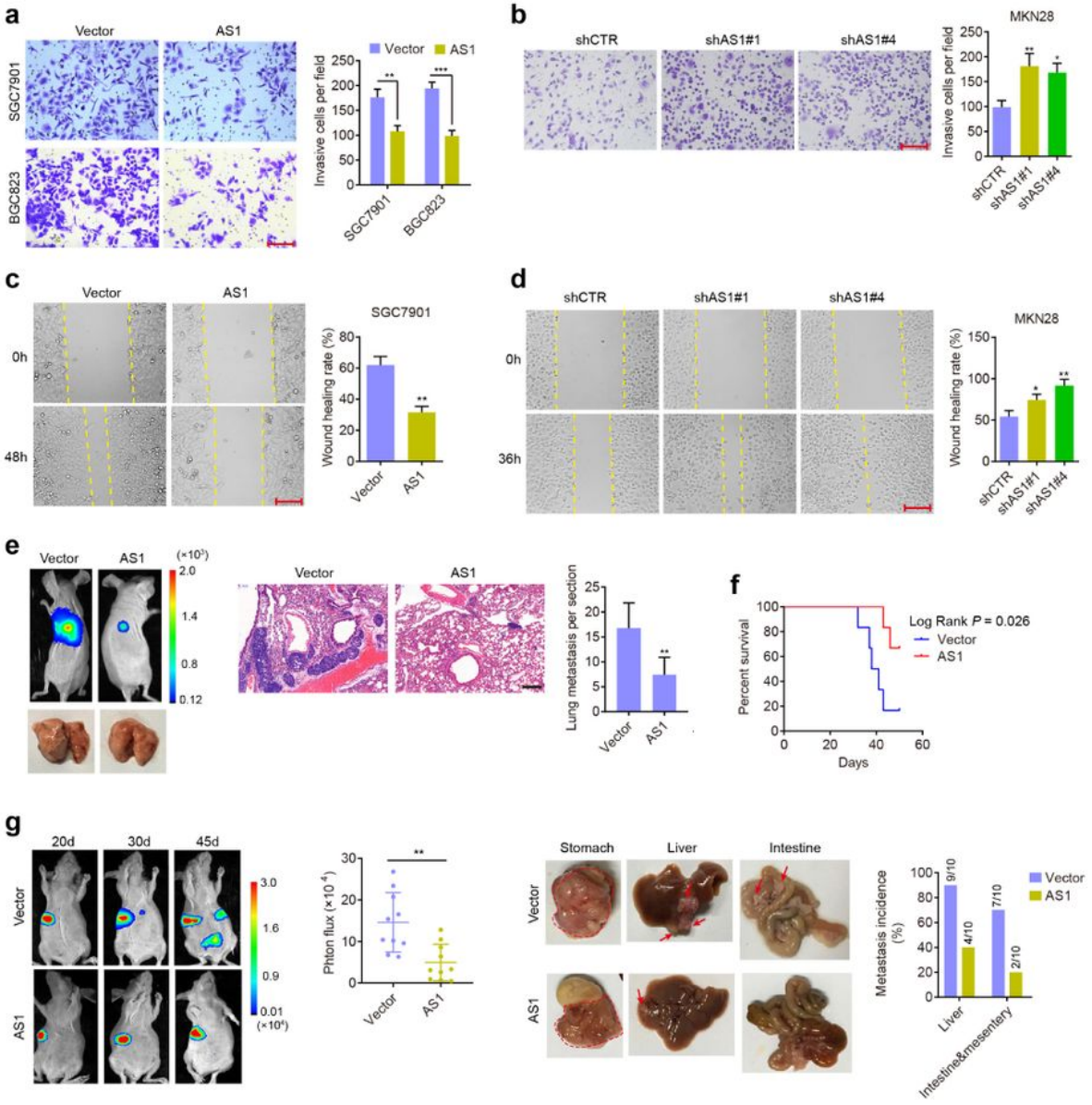

Figure 2

SGO1-AS1 suppresses invasive and metastatic activity of GC cells in vitro and in vivo. a-b. Transwell assay measuring cell invasion of SGC7901 and BGC823 cells stably expressing SGO1-AS1 (a), MKN28 cells stably silencing SGO1-AS1 (b) and their respective control cells. c-d. Wound-healing assay measuring the migratory ability of the indicated GC cells. a-d Scale bars, 150 μm. Error bars, SD from three independent experiments performed in triplicate. *P < 0.05, **P < 0.01, ***P < 0.001. e. SGC7901 cells stably expressing SGO1-AS1 or vector were intravenously injected into the tail-vein with nude mice. Representative bioluminescent images and H&E-stained lung sections of the mice are shown. The number of metastatic foci was quantified. Scale bar, 200 μm. Error bars represent SD (n = 5 mice/group). **P < 0.01. f. Kaplan-Meier survival curve for mice in a parallel experiment. g. SGO1-AS1 overexpressed SGC7901 cells, and the control cells were orthotopically injected into the stomach of nude mice (10 mice in each group). The mice were sacrificed 45 days later, and the tumor nodules in the abdominal cavity were examined. Representative IVIS luciferase in vivo images and bright views of liver and intestine isolated from the mice are shown. The Bioluminescence signal and number of mice with metastasis were quantified. **P < 0.01.

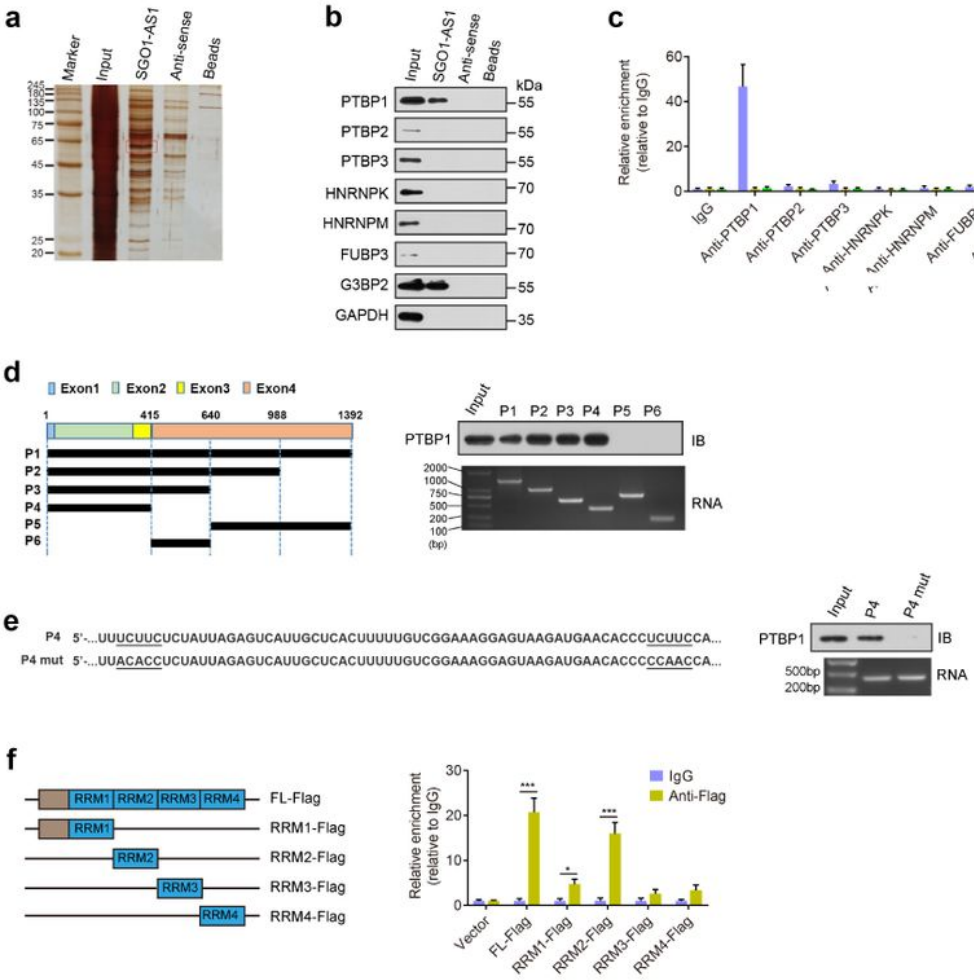

Figure 3

SGO1-AS1 RNA interacts with the PTBP1 protein. a. Identification of the SGO1-AS1-associated proteins by RNA pulldown assay. The proteins pulled down by SGO1-AS1 or the antisense RNA of SGO1-AS1 incubated with SGC7901cell extracts, were resolved by SDS-PAGE and subjected to silver staining. A specific band was identified in the SGO1-AS1 group and is marked with a red box. b. Western blotting validation of biotin-labeled RNA pulldown using sense or antisense probes in SGC7901 cells. GAPDH was

used as a negative control. c. RIP-qPCR detection of indicated RNAs retrieved by specific antibodies in MKN28 cells. The fold enrichment of SGO1-AS1 relative to IgG was determined by qRT-PCR. U6 RNA and GAPDH act as negative controls. d. Serial deletions of SGO1-AS1 were used in the RNA pulldown assays to identify the core regions of SGO1-AS1 that were required for physical interaction with PTBP1. Left panel: graphic illustration of SGO1-AS1 probes. e. RNA pulldown assay was performed using biotin-labeled 1-415 nt (P4), and PTBP1-binding site mutated RNA (P4 mut) of SGO1-AS1, followed by Western blotting. f. RIP assays were performed using an anti-Flag antibody in HEK293T cells transfected with Flag-tagged PTBP1 or its deletion mutants. qRT-PCR was used to measure the enrichment of SGO1-AS1. Error bars represent SD. *P < 0.05, ***P < 0.001.

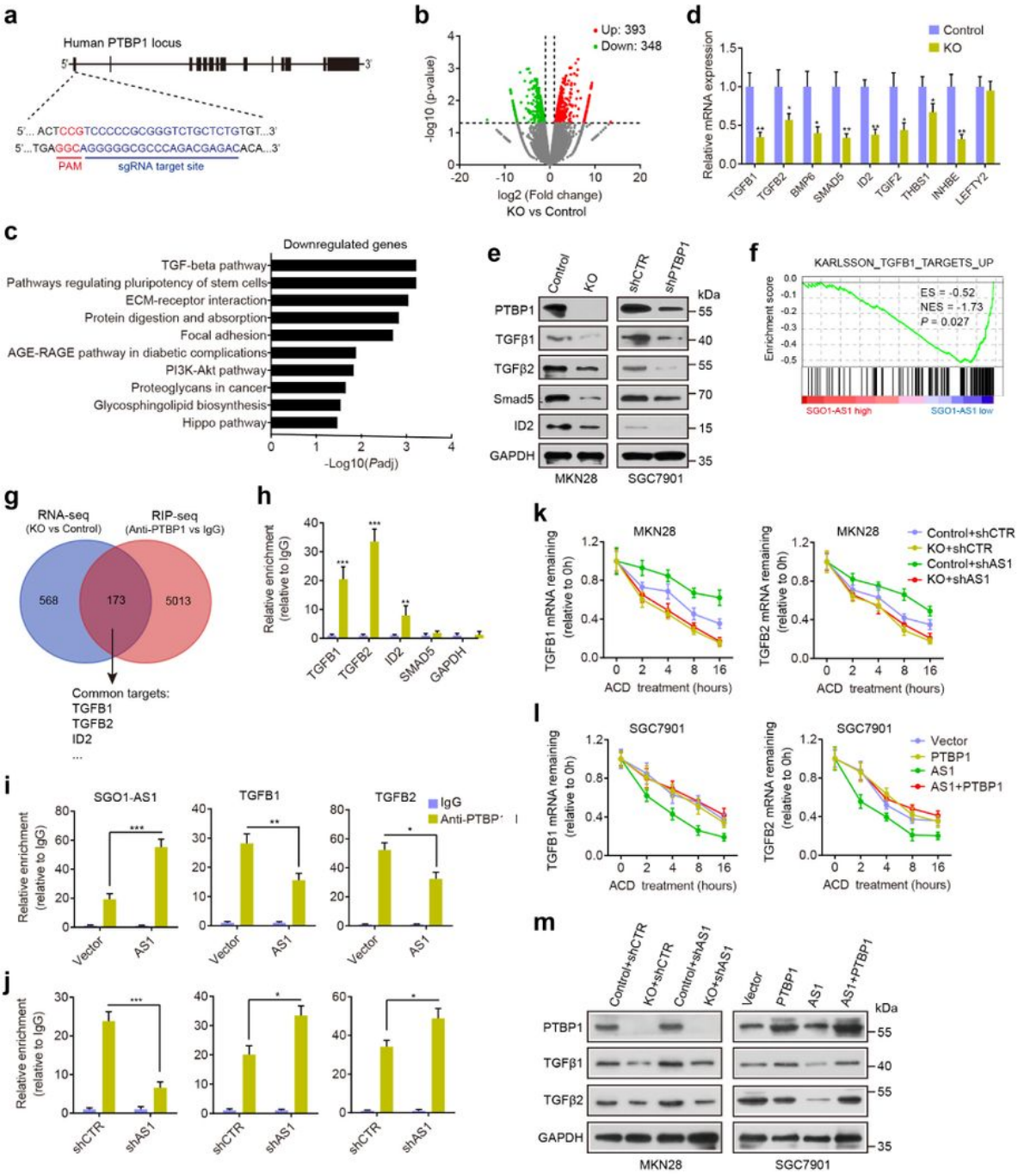

Figure 4

SGO1-AS1 promotes TGFB1/2 mRNA decay by interaction with PTBP1. a. PTBP1-knockout (KO) MKN28 cells were produced using the CRISPR/Cas9 system. Disruption of the PTBP1 locus. b. Volcano plots showing differentially expressed genes in PTBP1-KO vs. control cells. c. KEGG analysis of the downregulated genes in PTBP1-KO vs. control cells. d-e. qRT-PCR and Western blotting were used to validate the expression of genes involved in TGFβ pathway in the indicated cells. f. GSEA results plotted

to visualize the correlation between the expression of SGO1-AS1 and TGFβ target genes in TCGA stomach adenocarcinoma RNA-seq dataset. g. Overlay of differentially expressed genes following PTBP1 knockout and PTBP1-binding target mRNAs. h. PTBP1 RIP assay to analyze interactions between PTBP1 protein and TGFB1/2 or ID3 mRNA in MKN28 cells. The relative fold enrichment of these mRNAs compared to IgG was determined by qRT-PCR. SMAD5 and GAPDH served as the negative controls. i-j. The enrichment of SGO1-AS1 RNA and TGFB1/2 mRNA in PTBP1 immunoprecipitants was detected by RIP-qPCR assay in SGC7901 cells with SGO1-AS1 overexpression (i) or MKN28 cells SGO1-AS1 knockdown (j), respectively. k-l. TGFB1/2 mRNA stability assessment in the indicated cells treated with actinomycin D (5 μg/mL) for 2, 4, 8 and 16 h. The TGFB1/2 mRNA abundance relative to GAPDH quantified by qRT-PCR (n = 3 independent experiments). m. Western blotting analysis of TGFβ1/2 and PTBP1 protein levels in the indicated cells. Error bars represent SDs. *P < 0.05, **P < 0.01, ***P < 0.001.

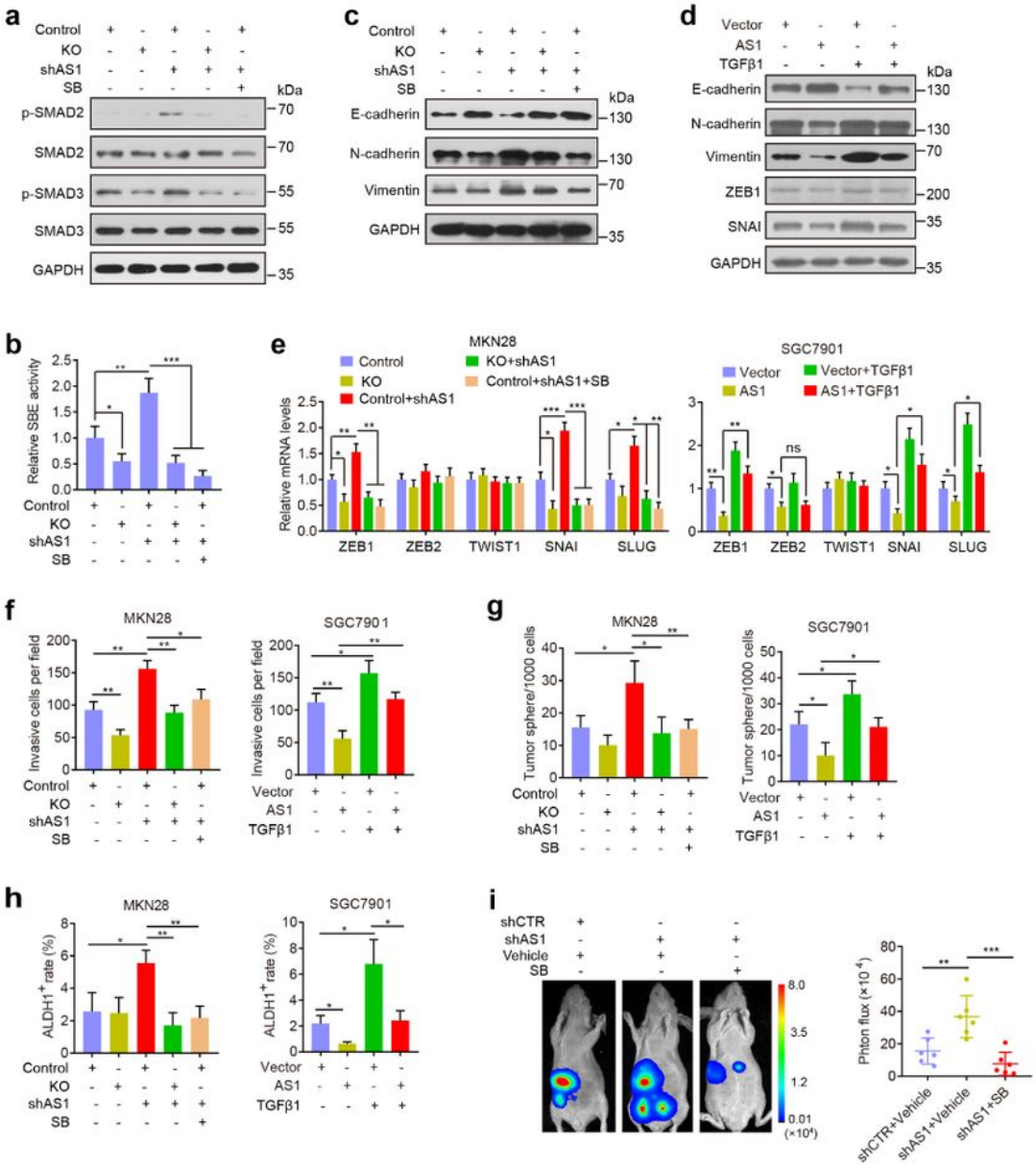

Figure 5

SGO1-AS1 impedes TGFβ signaling, EMT and stemness. a-b. SGO1-AS1 knockdown increased SMAD2/3 phosphorylation and SBE4 transcriptional activity and this effect was reversed by PTBP1 knockout or SB431542 (10 μM, 24 h), as shown by Western blotting (a) and luciferase reporter assays of the SBE4 promoter (b). c-d. EMT markers were measured in the indicated cells by Western blotting. e. qRT-PCR analysis of EMT-TFs expression in the indicated cells. f-h. Cell invasion ability (f), tumorsphere formation

efficiency (g) and rates of ALDH1 positive cells (h) in the indicated cells. i. MKN28 cells with SGO1-AS1 knockdown or control were orthotopically injected into the stomach of nude mice, and these mice were treated with PBS and SB431542 (20 mg/kg body weight, i.p) three times per week for 3 weeks (n = 6 mice per group). Tumor progression was monitored by luciferase signal intensity using an In Vivo Imaging System. Error bars indicate SDs. *P < 0.05, **P < 0.01, ***P < 0.001.

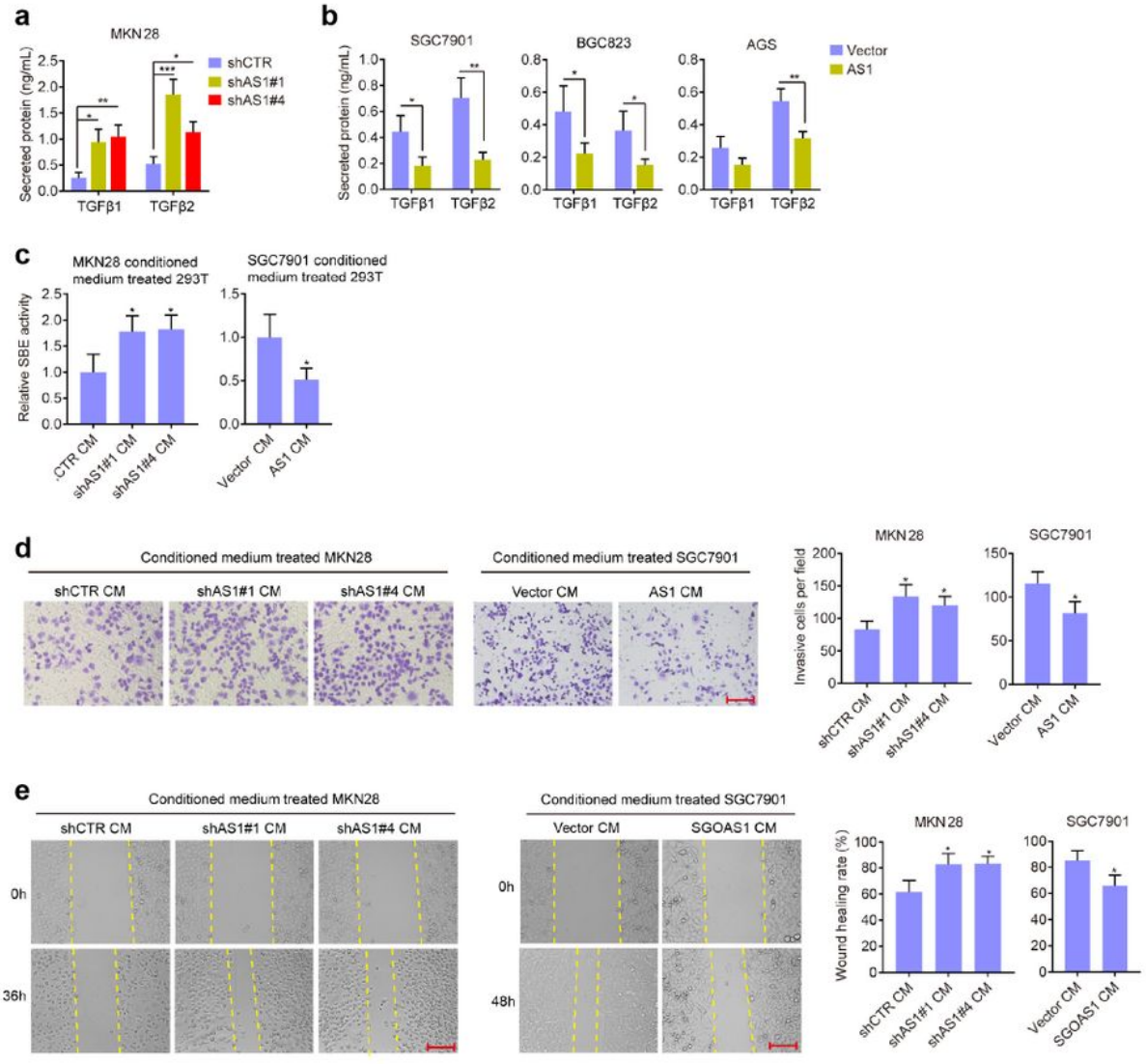

Figure 6

SGO1-AS1 decreases TGFβ autocrine. a-b. ELISA analysis of TGFβ1/2 protein levels in conditioned medium from the cells with SGO1-AS1 knockdown (a) or overexpression (b). c. Conditioned medium from SGO1-AS1-silencing MKN28 cells enhanced SBE4 promoter luciferase activity in HEK293T cells. Conversely, SBE4 transcription was downregulated in HEK293T cells with the administration of conditioned medium collected from SGO1-AS1-overexpressing SGC7901 cells compared to that collected from the control cells. d. Cell invasion ability of MKN28 cells increased when treated with conditioned medium from SGO1-AS1-silencing MKN28 cells, but that of SGC7901 cells was decreased upon treatment with conditioned medium from SGO1-AS1-overexpressing SGC7901 cells. e. Cell migratory ability of MKN28 cells was increased upon treatment with conditioned medium from SGO1-AS1-silencing MKN28 cells, while that of SGC7901 cells was decreased upon treatment with conditioned medium from SGO1-AS1-overexpressing SGC7901 cells. Scale bar, 150 μm. All error bars indicate SDs. *P < 0.05, **P < 0.01, ***P < 0.001.

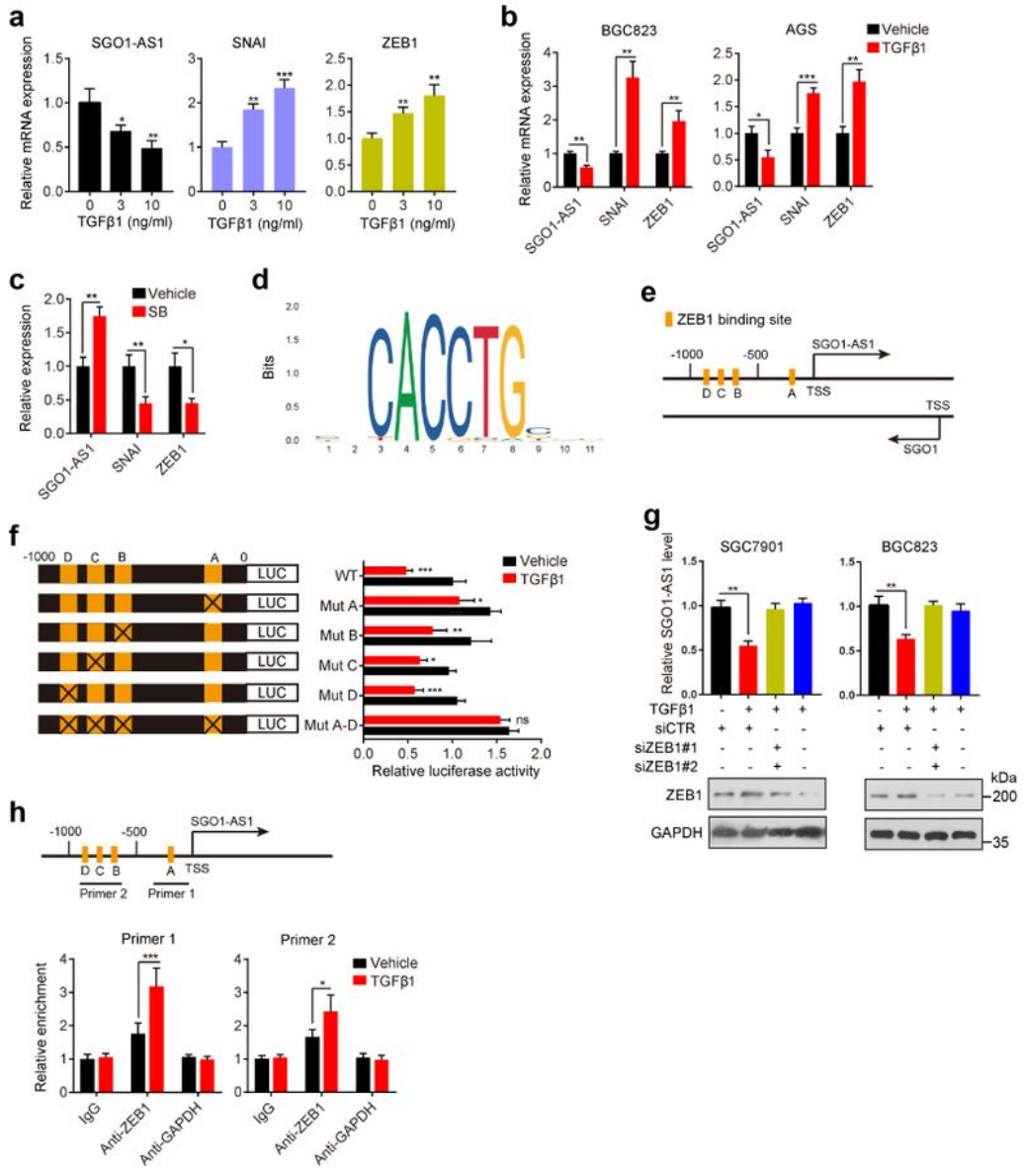

Figure 7

TGFβ downregulates SGO1-AS1 transcription via ZEB1. a. qRT-PCR analyses of SGO1-AS1, SNAI and ZEB1 levels in SGC7901 cells incubated with TGFβ1 (3 ng/mL or 10 ng/mL) for 24h. b. Expression levels of SGO1-AS1, SNAI and ZEB1 in BGC823 and AGS cells stimulated with 10 ng/mL TGFβ1 for 24 h. *P < 0.05, **P < 0.01 and ***P < 0.001 compared to those without TGFβ1 stimulation. c. SGO1-AS1, SNAI and ZEB1 levels in SGC7901 cells incubated with SB431542 (10 μM) for 24 h. *P < 0.05, **P < 0.01. d. The

recognition motif of ZEB1 from the JASPAR database (http://jaspar.genereg.net). e. A schematic diagram illustrating the four putative ZEB1 binding sites (Site A, B, C and D) in the SGO1-AS1 promoter. f. Luciferase report assays for the SGO1-AS1 promoter region containing either wild-type (WT) or mutated (Mut A, Mut B, Mut C, Mut D, Mut A-D) ZEB1 binding sites without or with TGFβ1 exposure. *P < 0.05, **P < 0.01, ***P < 0.001 and ns, not significant compared to without TGFβ1 stimulation. g. SGO1-AS1 expression was examined by qRT-PCR analysis in TGFβ1-treated SGC7901 and BGC823 cells transfected with ZEB1 siRNAs. Western blotting was performed to assess the inhibition efficiency in the same cells (right). **P < 0.01. h. Upper: Putative ZEB1-binding sites on SGO1-AS1 promoter region and design-indicated primers. Lower: ChIP analysis of ZEB1 enrichment on SGO1-AS1 promoter in SGC7901 cells treated with TGFβ1. IgG and anti-GAPDH antibodies were used as controls. *P < 0.05, ***P < 0.001. In all cases, error bars indicate SDs from three independent experiments.

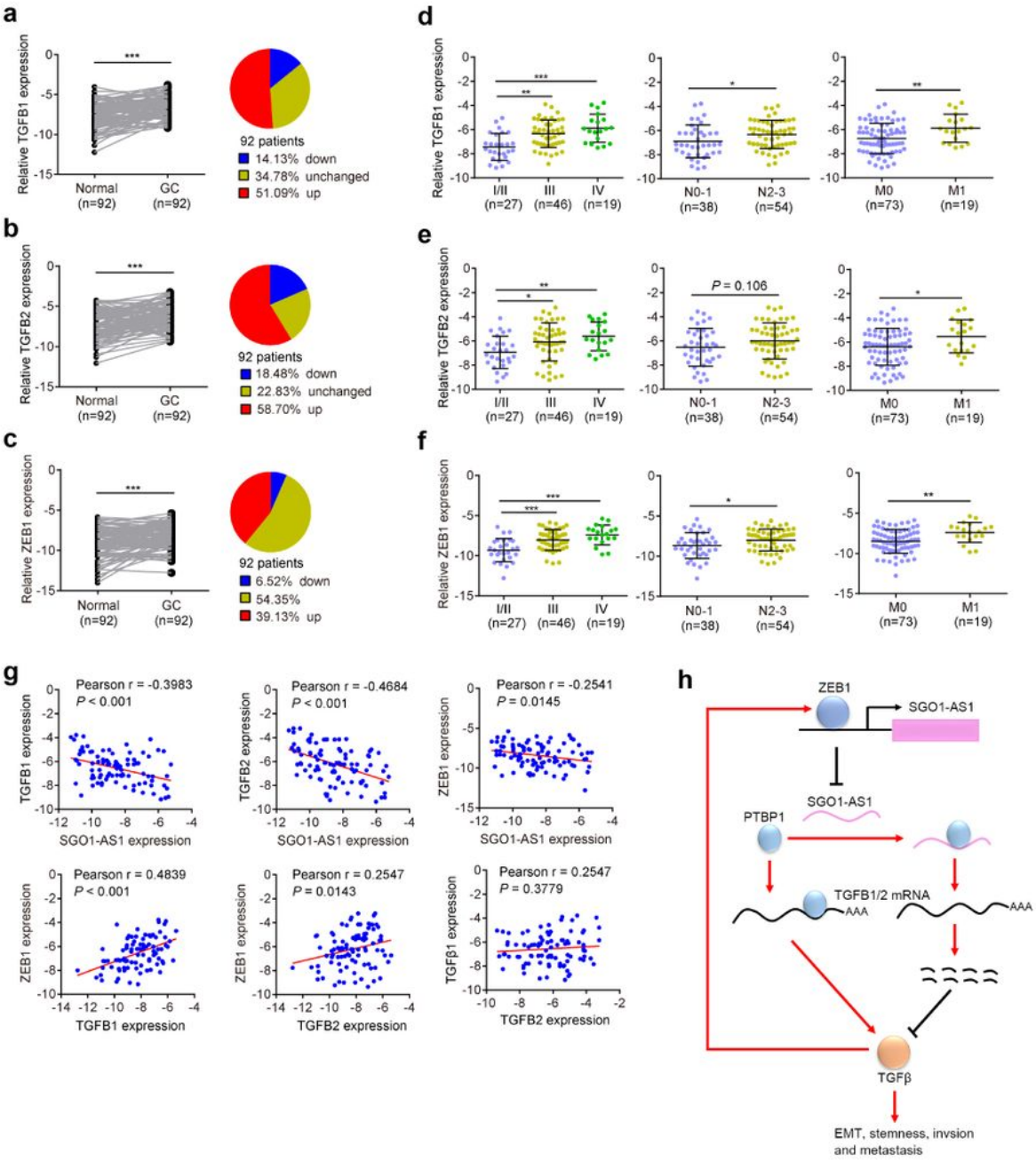

Figure 8

The expression levels of TGFB1/2 and ZEB1 and their correlations with SGO1-AS1 expression in GC tissues. a-c. Relative expression levels of TGFB1, TGFB2 and ZEB1 in 92 paired GCs and normal tissues from cohort 2 were quantified by qRT-PCR. The pie charts show the proportions of samples in the downregulation (blue), upregulation (red) and no change (yellow) categories. d-f. The expression levels of TGFB1, TGFB2 and ZEB1 in GCs according to their clinical stage and status of lymph node or distant

metastasis, respectively. g. SGO1-AS1 expression was inversely correlated with TGFB1, TGFB2 and ZEB1 expression, while ZEB1 expression was positively correlated with TGFB1/2 expression in the GC specimens. a-f, Error bars indicate SDs. *P < 0.05, **P < 0.01, ***P < 0.001. h. A schematic illustration of the TGFβ/ZEB1/SGO1-AS1 signaling pathway. TGFβ downregulates SGO1-AS1 by inducing ZEB1. SGO1-AS1 inactivates TGFβ signaling by promoting TGFB mRNA decay.

Supplementary Files

This is a list of supplementary files associated with this preprint. Click to download.

- Additionalfile1Supportinginformation.pdf